Indian Journal of Science and Technology, *Vol 9(37), DOI: 10.17485/ijst/2016/v9i37/85010, October 2016*
ISSN (Print) : 0974-6846
ISSN (Online) : 0974-5645

A Study on Fractal Based Image Compression in Modified HSI Space for Various Geometrical Topologies

Shimal Das[1]*, Dibyendu Ghoshal[2] and Jhunu Debbarma[1]

[1]Department of Computer Science& Engineering, Tripura Institute of Technology, Agartala, India; shimalcs.tit@gmail.com. jhunudb@gmail.com
[2]Departments of Electronics & Communication Engineering, National Institute of Technology, Agartala, India; tukumw@gmail.com

Abstract

A study on fractal geometry based image compression has been carried out in *Red-Green-Blue* (RGB), Hue Saturation Intensity (HIS) and modified HSI colour space and a comparative study has been carried out on Lena and Pine images. The modified HSI scheme incorporates the concept of non linearity in the saturation of the colour in the image. The non-linear model of HSI scheme is more realistic approach than the traditional HSI colour space. The output results have been obtained in the form of compressed image. In modified non-linear model, the processing speed and Peak Signal to Noise Ratio (PSNR) have been found to yield greater value compared to the other method but compression ratio has been obtained with lower values. The non-linear saturation, despite being a more realistic phenomenon, the self-similarity in the image may be lower and this may be considered as the major reason for lower compression ratio and higher processing speed.

Keywords: Fractal Compression, Hue Saturation Intensity (HSI) Space, Modified HSI Scheme, Red-Green-Blue (RGB) Space, Self-Similarity

1. Introduction

Fractal geometry has been found to be important for the compression of the images of irregular shape like snow bobs, clouds, arson, typhoon, tornado, hurricane, flame, tree leaves, mountain, and fountain etc[1]. The major strength of this technique lies in the inherent capacity to achieve high compression ratio and preserving ability of its original appearance following affine transformation.

Fractal coding is a lossy compression technique used normally for gray scale image through rectangular range and domain blocks[2]. The block segmentation may be conveniently achieved by quad tree sub-division approach which means the image plane is consecutively divided into four equal areas until matching is achieved between range and domain blocks. The matching has been achieved in order to get compression by iterated function system[3]. Subsequently a better algorithm based On Partition Iterated Function System (PIFS) was proposed[2] and it was found to yield higher and significant compression. In later stages, a number of studies[4-19], have been made to improve the coding efficiency and reducing the encoding time. In[20] a notable work has been done on color image for improving the quality of retrieved image during decoding of fractal images and whole coding approach was based on isosceles triangle segmentation instead of customary quad tree approach. Color imaging and processing have been gradually important with the advent of multimedia technology and internetworking system. The problem of color image is that it occupies at least three times more memory space compared to gray scale images for storage device which also needs higher processing time and transformation time or broad bandwidth of the transmission channel. Most common methods to encode

*Author for correspondence

a color image are to split the image it into red, green and blue channels and to compress them separately. The basic problem of *Red-Green-Blue* (RGB) color space is that the colour components are correlated with each other and signal intensity (Luminance part) and color content (Chrominance part) are co-related and indistinguishable even if one breaks them into three separate color channels.

In the present study, Hue Saturation Intensity (HSI) color space is taken to do fractal based compression of coloured. In this scheme hue contains various colours like red, green, blue, cyan, magenta, orange etc. and saturation indicates purity of color when intensity component is the gray level of the gray scale images.

In the standard HSI (HSV or HSB, or HSL) colour space, the variation of saturation in the colour image is considered to vary linearly. It renders further effect on visualization smoothness in colour purity distribution. In realistic case, saturation variation rarely occurs in a linear fashion. These come out of the factors of having the non linear property of colour sensor devices (like charge coupled device etc.) built in the digital cameras. The non-linear model may also occur due to thermal noises due to temperature variation on camera sensors. In the present study, three types of variation of colour saturation in the image plane have been studied, viz. sinusoidal, truncated exponential and truncated polynomial. These are not exhaustive, but only cited as possible choices. The relevant formulas for those have been presented in the following section. In the field of coloured image processing, already many researchers carried out their studies with HSI model with linear variation of saturation[21], but any study on coloured image compression using fractal based geometry is not described yet in the available reports.

Fractal coding of two color images have been done following quad tree and isosceles triangle based segmentation approach. It has been found that the proposed study has yielded better Peak Signal to Noise Ratio (PSNR), lower compression ratio and lower processing time.

The paper has been organized as follows:

Section 2 presents the mathematical formula related to fractal compression and compression for mile from RGB space to HSI space. Section 3 describes the proposed approach of compression done separately. Section 4 has shown the experimental results and Section 5 presents the conclusion and Section 6 presents the references.

2. Mathematical Background

2.1 Fractal Compression

A fractal may be represented by the set of equations[22]:

$$W\begin{bmatrix} x \\ y \end{bmatrix} = \begin{bmatrix} a & b \\ c & d \end{bmatrix}\begin{bmatrix} x \\ y \end{bmatrix} + \begin{bmatrix} e \\ f \end{bmatrix} \quad (1)$$

A fractal is generated when equation (1) is recursively iterated starting with an initial value of pixel location (x, y) on the image plane. The, a, b, c, d matrix indicates the rotation and skewing operations and e, f determine the translation of the image.

The set {w} is termed an affine transformation or contractive affine transformation. A fractal may be represented by a set of contractive affine transformation which are given by,

$$W_n P_n,\ n=1, 2, 3\ldots\ldots\ldots..N \quad (2)$$

Where W_n are the affine transformations and P_n denotes their individual importance. This representation is generally called IFS coding.

On self similarity concept in fractal based image compression, image blares are seen as rescale and intensely transformed approximate couples of block found elsewhere in the image plane. The compression ratio is proportional to the degree of self similarity.

The fractal image compression can be expressed by following steps:

Step 1: The image under test is partitioned into sub-images or range blocks. There may be different scheme to find such blocks, viz. quad tree partitioning, triangular partitioning, horizontal vertical partitioning, polygonal partitioning etc. The main aim in fractal compression is to partition an image into a smaller number of range blocks which should be similar to other portion of the image after undergoing different transformations.

Step 2: The searching of domain block should be done in a statistical manner. The purpose is to search for the best domain which will be mapped to a range. A domain is a region where the transformation mapping starts and a range is the region where it is mapped. If the best matched between the largest range blocks and the transformed domain blocks has got an error which is found to be greater than the similarity threshold (Based on some heuristic knowledge). The range

blocks should have similarly with each of these blocks. Range blocks which cannot be matched within the similarity threshold continue to partition into smaller range cells until the maximum number of partition is obtained. If this limit is touch and the nearest domain cell does not match a range cell within the said threshold. This area can be termed as anomalous area.

Step 3: When the matching with location is found, various transformations like combination of affine and luminance transformation are to be computed. The same can be represented as follows:

$$W\begin{pmatrix} x \\ y \\ z \end{pmatrix} = \begin{pmatrix} a & b & \mathbf{0} \\ c & b & \mathbf{0} \\ 0 & 0 & p \end{pmatrix} \begin{pmatrix} x \\ y \\ z \end{pmatrix} + \begin{pmatrix} e \\ f \\ q \end{pmatrix} \quad (3)$$

Here z indicates the pixel intensity (luminance) at the location (x, y), and e and f indicate the shift in the position of the range with respect to the domain p and q are the contrast and luminance adjustment to accomplish the affine transformation.

Step 4: The foundation of fractal image compression lies in the construction of the IFS that approximates the original image. An IFS in terms of set theory and distance function, is a union of contractive transformation each of which maps into itself. To realize contractive transformation, the following condition should hold good:

$$d\,(W\,(P_1),\, W\,(P_2)) < d\,(P_1,\, P_2) \quad (4)$$

The above equation is true for any metric space.

2.2 RGB to HSI Conversion and HSI to RGB Conversion

HSI stands for Hue, Saturation and Intensity. Hue represents dominant color as perceived by an observer[23]. It is a property associated with the dominant wavelength. Saturation refers to the relative purity of the amount of white light mixed with the color content. Intensity reflects the brightness. HSI decouples the intensity information from the color, while hue and saturation correspond to human perception, thus making this representation very useful for developing image processing algorithms. HSI color space is a popular color space because it is based on human color perception.

Figure 1 shows the double cone HSI color model. This HSI color model can be considered as a double cone, where S, θ, and I are indicates the saturation, hue and intensity respectively.

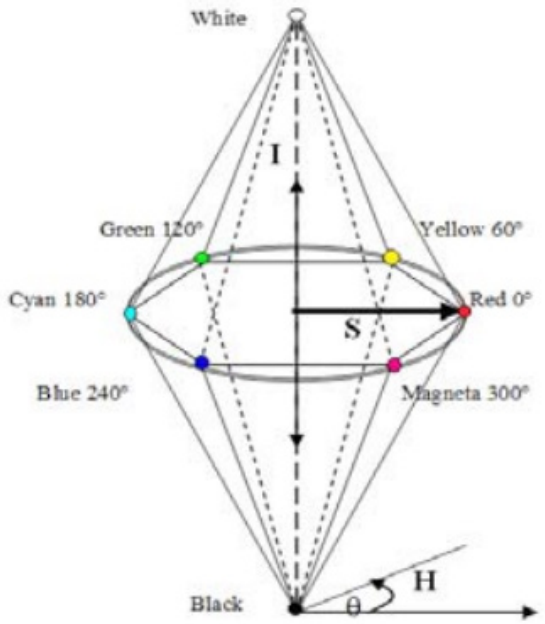

Figure 1. Representation of double cone HSI color model.

The conversation from RGB space to HSI space is given below

$$I = \frac{\mathbf{1}}{\mathbf{3}}\,(R + G + B) \quad (5)$$

$$S = \mathbf{1} - \frac{\mathbf{3}}{(R + G + B)[\min(R, G, and\ B)]} \quad (6)$$

$$H = \cos^{\dagger}(-1)\{(0.5[(R-G)+(R-B))/\sqrt{([(R-G)\square^{\dagger}2+(R-B)(G-B))}\} \quad (7)$$

Converting colors from HSI to RGB, there are three applicable equations depend on the values of H. Three sectors are lying 120°angular interval in the separating primes.

RG sector (0°≤ H < 120°): When H is this sector, the RGB components are given by the equations as

$$B = I(\mathbf{1} - s) \quad (8)$$

$$R = I\left[1 + \frac{ScosH}{\cos(60^0 - H)}\right] \quad (9)$$

$$G = \mathbf{3}I - (R + B) \quad (10)$$

GB sector (120°≤ H < 240°): If the given value of H is in this sector, we first subtract 120° from it:

$$H = H - 120° \tag{11}$$

Then the RGB components are

$$R = I(1 - s) \tag{12}$$

$$G = I\left[1 + \frac{ScosH}{\cos(60^0 - H)}\right] \tag{13}$$

$$B=3I-(R + G) \tag{14}$$

BR sector (240°≤ H < 360°): Finally, if H is in this range, we subtract 240° from it:

$$H = H - 240° \tag{15}$$

Then the RGB components are:

$$G = I(1 - s) \tag{16}$$

$$B = I\left[1 + \frac{ScosH}{\cos(60^0 - H)}\right] \tag{17}$$

$$R = 3I - (G + B) \tag{18}$$

2.3 Assumption for Non-Linear Saturation Model

The non-linear saturation of colour is assumed to be represented by the three following expressions:

$$\frac{\sin\theta}{max} = 1 \tag{19}$$

Where $\theta = \{\theta: 0,1\}$

$$e^{-x} = 1 - x + \frac{x^2}{2!} - \frac{x^3}{3!} + \frac{x^4}{4!} \cdots \cdots \cdots \tag{20}$$

$$y = f(x) = a_0 + a_1x + a_2x^2 + \cdots + a_nx^n \tag{21}$$

It is known to the scientist community that in most of the natural or uncontrolled event are basically non linear in nature whereas the linear variation of such an event or quality is an idealistic concept. Saturation of colour in any colour image varies from 0 to 1 and in realistic case; they do not vary in a linear manner with respect to space. The non linearity has been modeled in the present paper in three ways. The variation in first case is sinusoidal which, although may not be frequently realizable, still its range of variation falls within the describable range i.e. from 0 to 1. In the second case, exponential variation with negative exponent maximum value of saturation would be found at the periphery of the cone model of HSI scheme. Saturation value will decrease exponentially depending on the value of the exponent. Formula dictates that higher value of exponent would lead to fall of saturation at faster rate. The third formula shows a polynomial where the values of coefficients a_n's would ultimately decide the fall. Further, the value of saturation does not necessarily fall to zero value at the axis of the cone and it is valid for all the above three cases.

3. Proposed Method for Fractal Coding Based on Quad-tree and Isosceles Triangle Segmentation

Hue Saturation intensity color space is an uncorrelated system unlike to RGB system. Here only scope for fractal compression is to treat each channel separately followed by the standard fractal compression algorithm. The range and domain blocks are chosen according to two geometric dimensions viz. quad tree and isosceles triangle based segmentation.

The geometric affine transformation is carried out according to the equations (2) and intensively transformation is done by taking the average value of two neighborhood pixels of the matched shrink image. For isosceles triangle segmentation method, the earlier

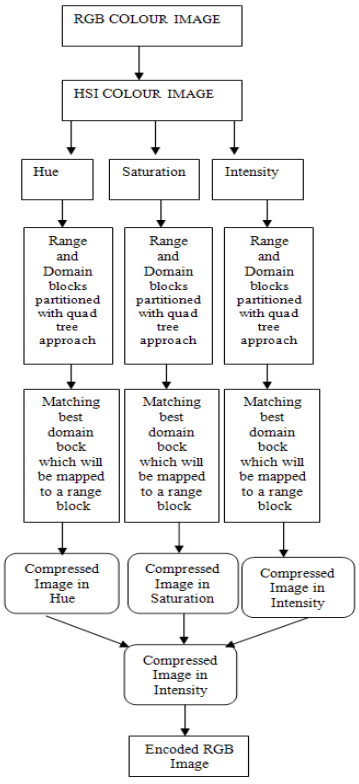

Figures 2 (a). The color image encoding process based on HSI and quad tree approach

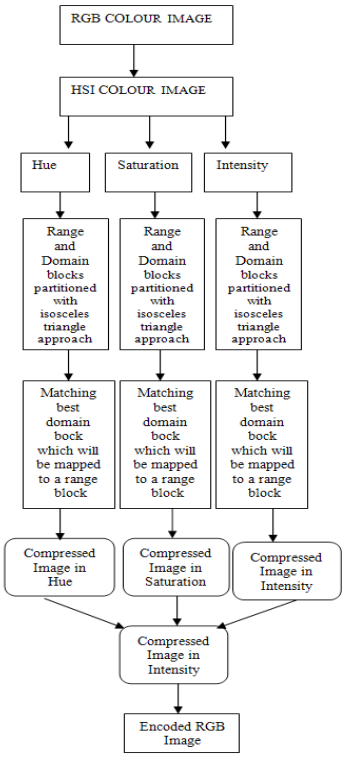

Figures 2 (b).The color image encoding process based on HSI and Isosceles triangle segmentation

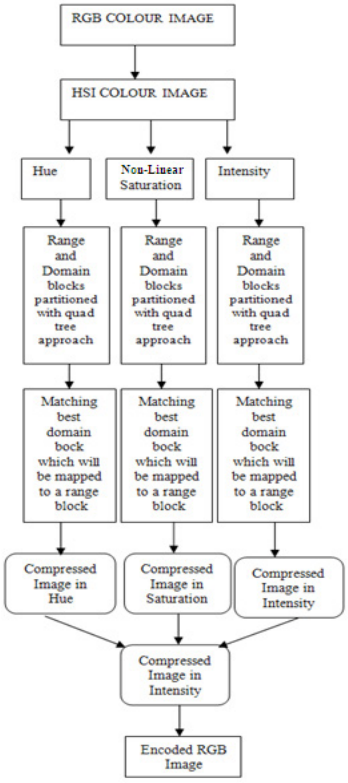

Figures 2 (c).The color image encoding process based on modified HSI with quad tree approach

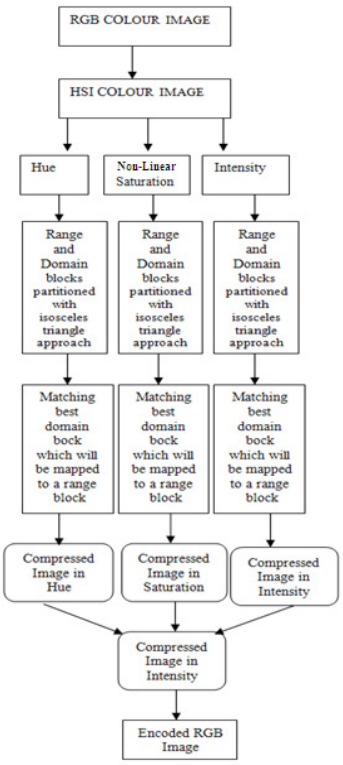

Figures 2 (d). The color image encoding process based on modified HSI and Isosceles triangle segmentation

method of[20] is followed. Here the compression process is carried out for each channel and this also entails non-linear saturation channel. The operation is done independently as HSI space does not involve any interdependence or co-relation between the channels. The computation time is in HSI space is smaller than that obtained in RGB schemes where processing of fractal coding was done separately i.e. without considering the co-relation between them. Images were decoded according to the method of[20] as it can easily be applicable for both quad tree and triangular segmentation approaches. Figure 2 (a), (b), (c) and (d) show the color image encoding process based on HSI with quad tree approach, encoding process based on HSI with Isosceles triangle segmentation, encoding process based on modified HSI with quad tree approach, and encoding process based on modified HSI with Isosceles triangle segmentation respectively.

4. Results and Discussions

The proposed method has considered two digital images viz. Lena and pine (256× 256 ×3) to enable comparison with the earlier studies. The simulation work has been

come out with Mat lab 2014 b in Windows 7 operating system.

Original and compressed image of Lena, original and compressed image of Pine have been shown in Figures-3(a), 3(b), 3(c), and 3(d), respectively for quad tree approach. The original and compressed image of Lena, original and compressed Pine images following isosceles triangle geometry have been shown in Figures 4(a), 4(b), 4(c) and 4(d), respectively. The decoded images of Lena and Pine are shown in Figures 5 and 6.

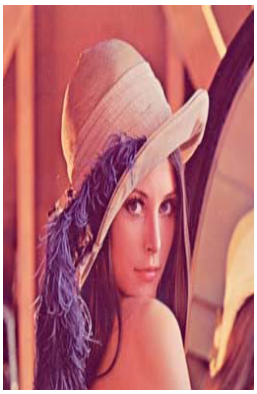

3(a)

(3b)

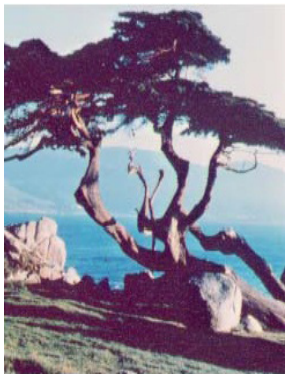

3(c)

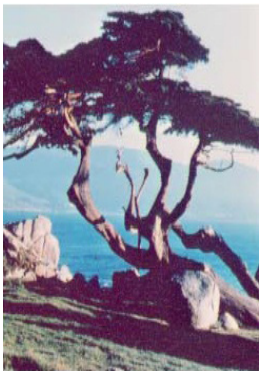

3(d)

Figure 3. (a), (c) The original images of Lena and Pine, (b) and (d) the compressed images of Lena and Pine for quad tree approach and based on HSI model

4(a)

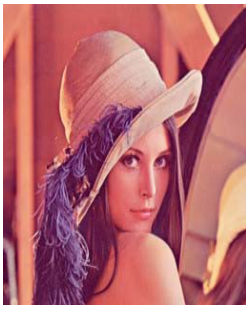

4(b)

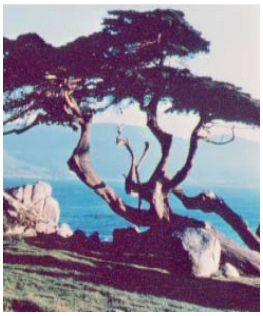

4 (c)

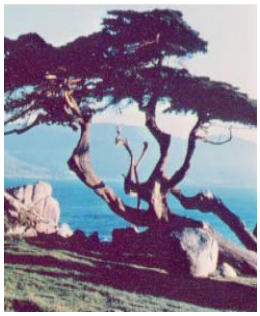

4(d)

Figure 4. (a) The original image of Lena, (b) the compressed image of Lena, (c) show the original image of Pine and (d) the compressed image of Pine for Isosceles triangle approach

Figures 5 (a) and (b) show the original images, Figures 5 (c) and (d) show the composite image and Figures 5 (e) and (f), show the retrieved images of Lena and Pine for HIS with quad tree approach. More over Figures 6 (a) and (b) show the original images, Figures 6 (c) and (d) show the composite and Figures 6 (e) and (f) show the retrieved images of Lena and Pine for HSI with Isosceles Triangle approach.

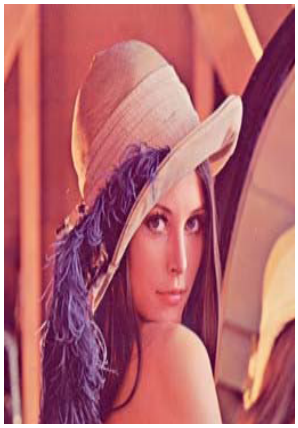

5(a)

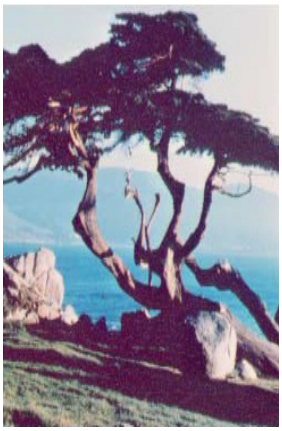

5(b)

5(c)

5(d)

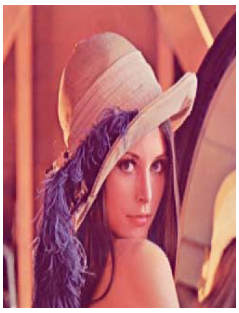

5(e)

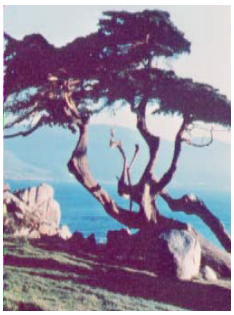

5(f)

Figure 5 (a), (b). The original images Lena and Pine, (c), (d) the composite images of Lena and Pine and (e), (f) the retrieved images of Lena and Pine for HSI with quad tree approach

6(a)

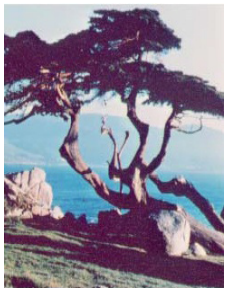

6(b)

6 (c)

6(d)

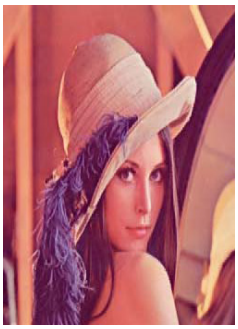

6(e)

6(f)

Figures 6. (a) (b) The original images of Lena and Pine, (c), (d) the composite images of Lena and Pine and (e), (f) the retrieved images of Lena and Pine for HSI with Isosceles triangle approach

Figures 7 (a) and (b) show the original images, Figures 7 (c) and (d) show the composite image and Figures 7 (e) and (f), show the retrieved images of Lena and Pine for modified HIS with quad tree approach. More over Figures 8 (a) and (b) show the original images, Figures 8 (c) and (d) show the composite and Figures 8 (e) and (f) show the retrieved images of Lena and Pine for modified HSI with Isosceles Triangle approach.

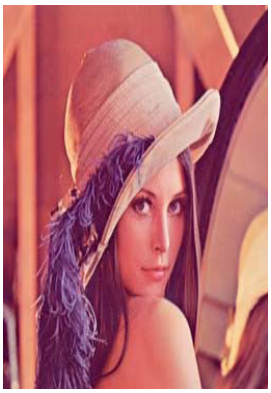

7(a)

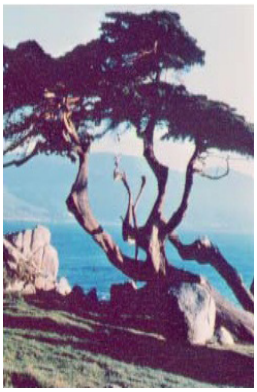

7(b)

7(c)

7(d)

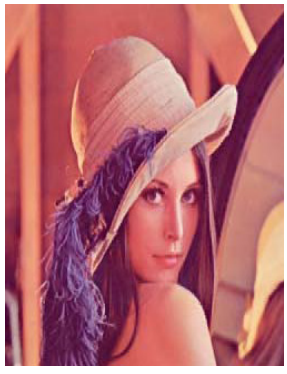

7(e)

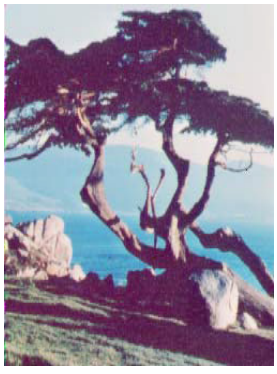

7 (f)

Figure 7 (a), (b). The original images Lena and Pine, (c), (d) the composite images of Lena and Pine and (e), (f) the retrieved images of Lena and Pine for modified HSI with quad tree approach

8(a) 8(b)

8 (c) 8(d)

8(e) 8(f)

Figures 8. (a) (b) The original images of Lena and Pine, (c), (d) the composite images of Lena and Pine and (e), (f) the retrieved images of Lena and Pine for modified HSI with Isosceles Triangle approach

Although the emphasis of the present study was laid down on the efficiency of compression using fractal geometry, image recovery was also achieved to verify the strength of the algorithms involved and their applicability. The quality of image is evaluated by PSNR[24]. PSNR is calculated by the following equation.

$$\mathbf{PSNR} = \mathbf{10}\ \mathbf{log_{10}} \frac{\mathbf{255^2}}{\left(\frac{1}{m*n}\right)\sum_{c=1}^{M}\sum_{j=1}^{N}(Xi,j - \hat{X}i,[j])^2} \quad (22)$$

Where M×N is the size of the image, *Xij* and $\hat{X}ij$ *are the* pixel values of original and reconstructed image at position (i,j). Normally better image quality implies larger value of PSNR.

The results are shown in Table 1 PSNR, encoding time and compression ratio using the proposed and earlier methods.

As shown in the Table 1, the proposed method has lower processing time and lower compression ratio compared to those obtained by[2] where 4×4 size for block segmentation was followed. The isosceles triangle method has far better compression ratio and PSNR for H, S and I components. The processing time is also found to be less in normal HSI scheme for 4×4 block and triangle geometry. Out of these, the latter has produced better perform parameters. As compression ratio slightly values intensely with the number of range blocks, the compression ratio is found to be slightly higher in the approach of Jaquin where the number of square range blocks were much less than the triangular block approach. Still, HSI scheme out performs separate RGB scheme in term of PSNR, processing time and compression ratio.

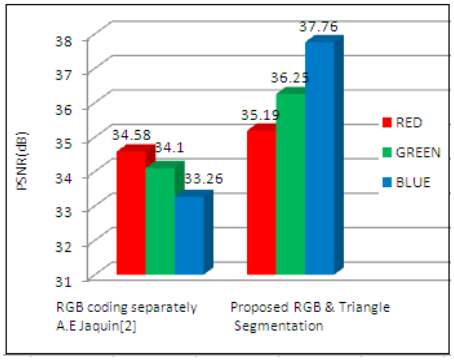

Figures 9. PSNR (dB) for Lena image at RGB coding separately[2] and proposed method (RGB with triangle segmentation) approach

The results obtained by modified HSI space, it is found that the PSNR value and processing time are higher compared to those obtained by normal HSI space; but the compression ratio is found to be lower in modified HSI space (for all three polynomial wise variation approach). This is evident as the non-linearity in saturation of colour would, in twin, give more dissimilarity with respect to colour in the coloured image.

Figure 9 shows the comparison of PSNR (dB) for Lena in RGB space (coding separately)[2], and proposed method (RGB and Triangle segmentation).

From the comparative results in Figure 9, it has been found that in proposed method (RGB and Triangle segmentation) the value of PSNR (dB) for Lena is increased compared to RGB space (coding separately)[2].

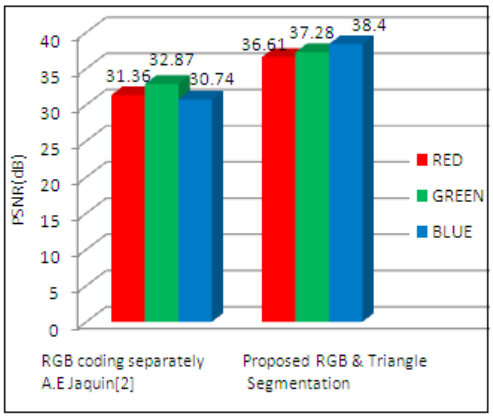

Figures 10. PSNR (dB) for Pine at RGB coding separately[2] and proposed method (RGB with triangle segmentation) approach

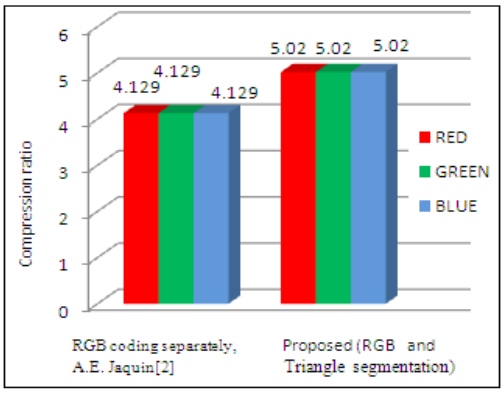

Figures 11. Comparison chart of compression ratio for Lena image at RGB coding separately[2] and proposed method (RGB with triangle segmentation) approach

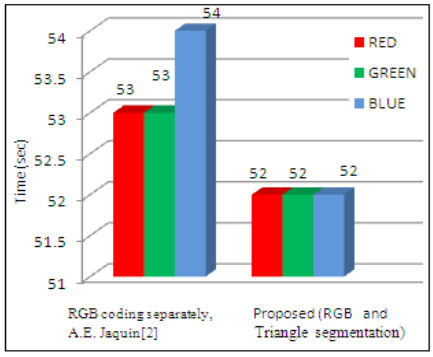

Figures 12. Chart of compression time (sec) for Lena image at RGB coding separately[2] and proposed method (RGB with triangle segmentation) approach

Figure 10 Shows the comparison chart of PSNR (dB) for Pine image in RGB coding separately[2], and proposed method (RGB and triangle segmentation) approach. From the comparison chart it has been noticed that PSNR (dB) for Pine image is slightly enhanced in proposed method compared to RGB space (coding separately)[2] method.

From Figure 11, it has been observed that the compression ratio of Lena image is higher in Proposed method (RGB and Triangle segmentation) approach than RGB space (coding separately)[2].

Figure 12 Shows the of compression time (sec) for Lena image at RGB coding separately[2], and Proposed method (RGB and Triangle segmentation) approach. From the comparison chart it has been observed that less compression time (sec) required for Lena image in proposed techniques compared than RGB space (coding separately)[2] approach.

Figure 13 Shows the of compression time (sec) for Pine image at RGB space (coding separately)[3] and Proposed method (RGB and Triangle segmentation) approach.

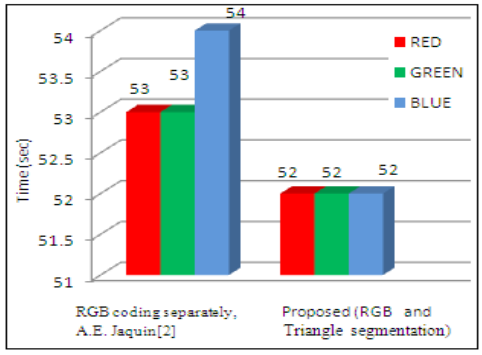

Figures 13. Chart of time (sec) for Pine image at RGB coding separately[2] and proposed method (RGB with triangle segmentation) approach

From the comparison chart, it is seen that the compression time (sec) needed for Pine image is less in proposed techniques compared with RGB space (coding separately)[2] approach.

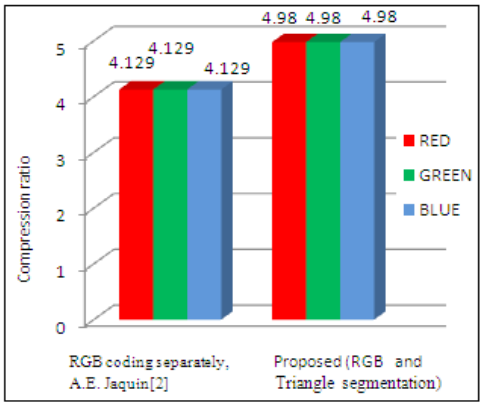

Figures 14. Chart of compression ratio for Pine image at RGB coding separately[2] and proposed method (RGB with triangle segmentation)

Table 1. Comparison between RGB (Separately), HSI method (Proposed) and modified HIS (proposed) based on Quad-Tree and Isosceles triangle code block segmentation

i) RGB Based Segmentation Approach

RGB coding separately, A.E. Jaquin[2]					Proposed method (RGB and Triangle segmentation)		
Test images	**RGB**	**PSNR (dB)**	**Time (sec)**	**Compression ratio**	**PSNR (dB)**	**Time (sec)**	**Compression ratio**
Lena	R	34.58	53	4.129	35.19	52	5. 02
	G	34.10	53		36.25		
	B	33.26	54		37.76		
Pine	R	31.36	58	4.129	36.61	54	4.98
	G	32.87	53		37.28		
	B	30.74	54		38.4		

ii) HSI Based Segmentation Approach

Proposed method HSI scheme(quad tree)					Proposed method HSI scheme (Triangle segmentation)		
Test images	**HSI**	**PSNR (dB)**	**Time (sec)**	**Compression ratio**	**PSNR (dB)**	**Time (sec)**	**Compression ratio**
Lena	H	35.12	44	23.13	36.47	43	26.78
	S	34.70	42	24.51	37.20	41	27.87
	I	33.42	41	23.72	38.10	42	26.75
Pine	H	32.52	44	22.68	33.10	42	24.62
	S	33.88	42	24.98	36.83	43	25.79
	I	30.92	41	25.72	38.14	41	28.88

iii) Modified HSI Scheme Based Segmentation Approach

Proposed modified HSI scheme(quad tree)					Proposed modified HIS scheme (Triangle segmentation)		
Test images	**Non-linear saturation**	**PSNR (dB)**	**Time (sec)**	**Compression ratio**	**PSNR (dB)**	**Time (sec)**	**Compression ratio**
Lena	Sinusoidal	37.18	39	22.12	38.22	41	25.56
	Exponential	35.22	38	23.10	39.42	38	25.76
	Polynomial	34.18	39	22.20	39.10	39	24.84
Pine	Sinusoidal	36.31	38	21.32	35.90	39	24.11
	Exponential	37.43	39	23.34	38.76	38	24.12
	Polynomial	34.11	39	23.54	39.88	38	26.44

From Figures 14, it is clear that compression ratio slightly increased for Pine image in proposed method (RGB and Triangle segmentation) approach compared than RGB space (coding separately)[2].

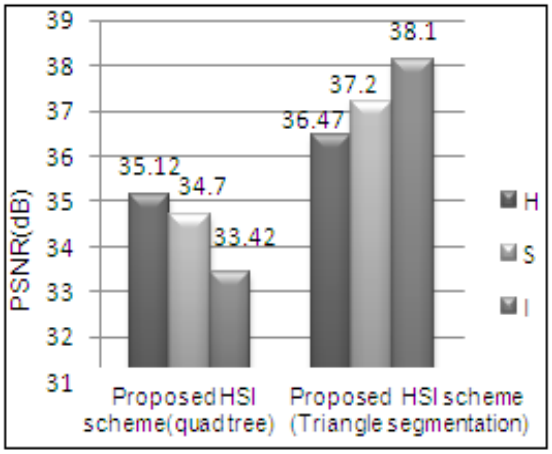

Figures 15. Chart of PSNR (dB) for Lena image in proposed HSI scheme (quad tree) and proposed HSI scheme (triangle segmentation)

Figures 15 shows the comparison chart of PSNR (dB) for Lena image in proposed HSI scheme (quad tree) and Proposed HSI scheme (Triangle segmentation), Figures 16, 18 and 20 show comparison chart of PSNR (dB) and comparison chart of time (sec) and comparison chart of Compression ratio for Lena image in proposed HSI scheme (quad tree) and Proposed HSI scheme (Triangle segmentation). Figures 17 and 19 display comparison chart of time (sec) and compression ratio for Lena image in proposed HSI scheme (quad tree) and proposed HSI scheme (Triangle segmentation) approaches.

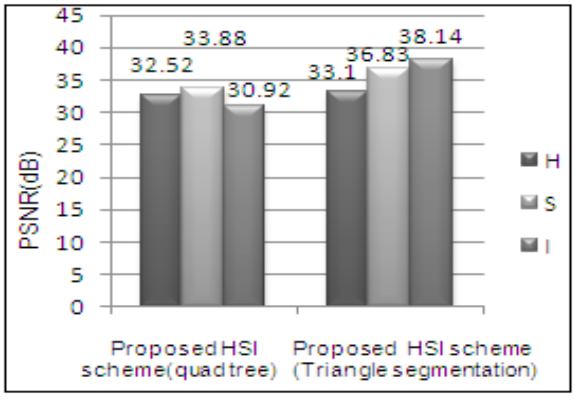

Figure 16. Chart of PSNR (dB) for Pine image in proposed HSI scheme (quad tree) and proposed HSI scheme (triangle segmentation)

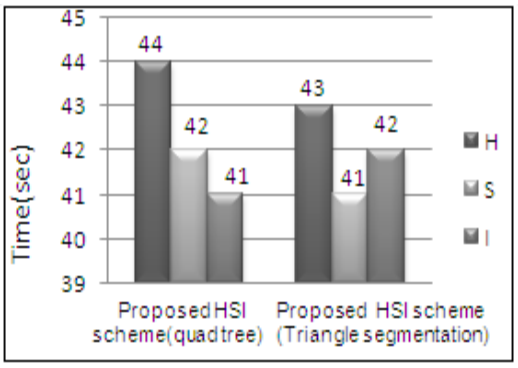

Figure 17. Chart for processing time (sec) for Lena image in proposed HSI scheme (quad tree) and proposed HSI scheme (triangle segmentation)

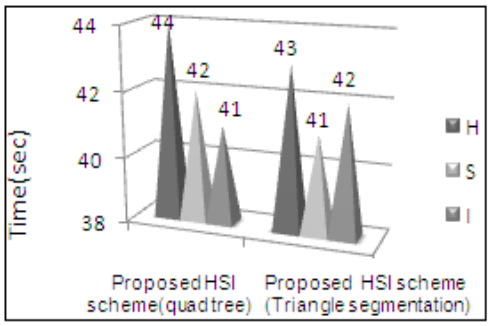

Figure 18. Chart for processing time (sec) for pine image in proposed HSI scheme (quad tree) and proposed HSI scheme (triangle segmentation)

Figures 21and 22 show the compression ratio for Lena image and compression ratio for Pine image in: 1. RGB space (coding separately)[2], 2. proposed method (RGB and triangle segmentation) approach, 3. proposed HSI scheme (quad tree), and 4. proposed HSI scheme (triangle segmentation) respectively.

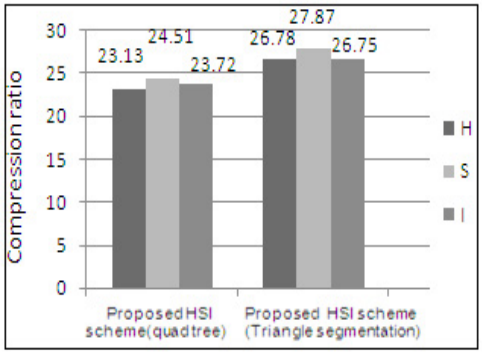

Figure 19. Compression ratio for Lena image in proposed HSI scheme (quad tree) and proposed HSI scheme (triangle segmentation)

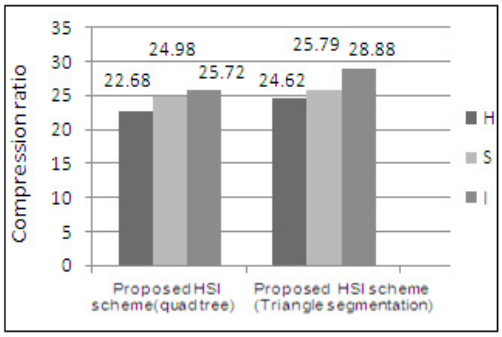

Figure 20. Compression ratio for pine image in proposed HSI scheme (quad tree) and proposed HSI scheme (Triangle segmentation)

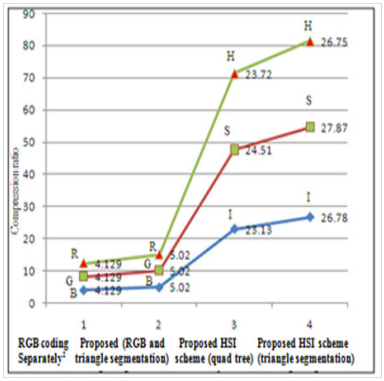

Figures 21. Compression ratio for Lena image in (1) RGB coding separately[2], (2) proposed method (RGB and triangle segmentation), (3) proposed HSI scheme (quad tree) and (4) proposed HSI scheme (triangle segmentation)

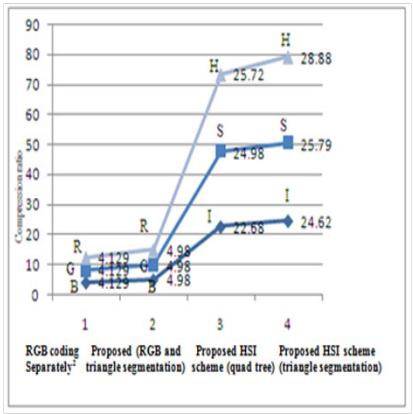

Figures 22. Compression ratio for Pine image in (1) RGB coding separately[2], (2) proposed method (RGB and triangle segmentation), (3) proposed HSI scheme (quad tree) and (4) proposed HSI scheme (triangle segmentation)

Figure 23 shows the PSNR value for Lena and Pine images for proposed modified HSI scheme (quad tree) and proposed modified HSI scheme (triangle segmentation), respectively. Figure 24 shows the compression ratio for Lena and Pine images for proposed modified HSI scheme (quad tree) and proposed modified HSI scheme (triangle segmentation) respectively and Figures 25 shows the execution time for Lena and pine images for proposed modified HSI scheme (quad tree) and proposed modified HSI scheme (triangle segmentation), respectively.

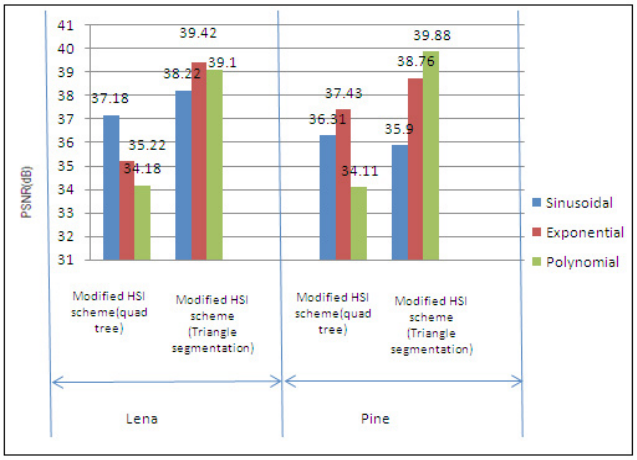

Figures 23. PSNR for proposed modified HSI scheme (quad tree) and proposed modified HSI scheme (triangle segmentation) for both Lena and Pine images separately

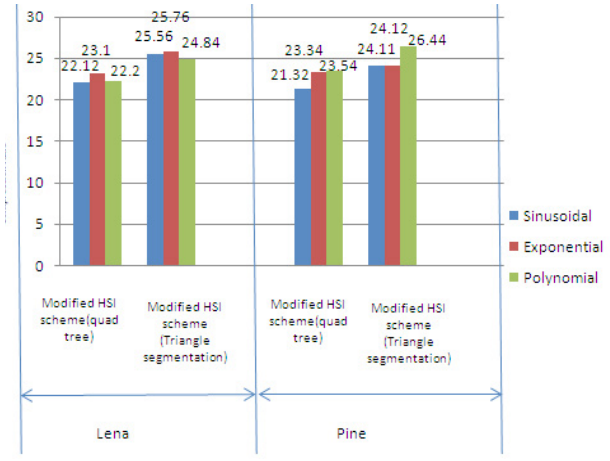

Figures 24. Compression ratio for proposed modified HSI scheme (quad tree) and proposed modified HSI scheme (triangle segmentation) for both Lena and Pine images separately

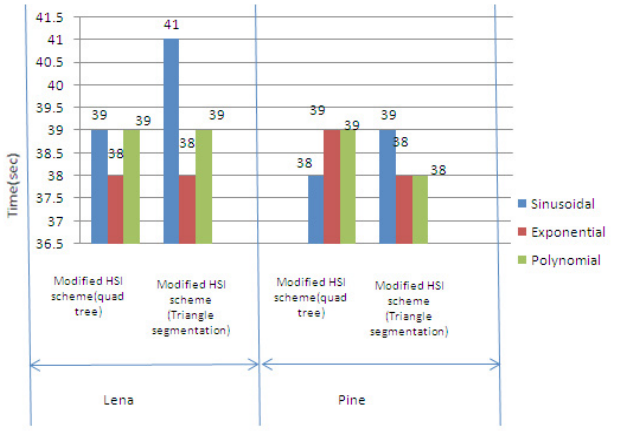

Figures 25. Execution time for proposed modified HSI scheme (quad tree) and proposed modified HSI scheme (triangle segmentation) for both Lena and Pine images separately

5. Conclusion

In the proposed scheme of colour image compression, the figure of merit like PSNR (with respect to the processed image compared to the unprocessed image) does not show remarkable improvement when isosceles triangle based segmentation is taken. Compression ratio is also increased marginally and it may occur due to the dual complexity of the RGB colour scheme and partitioned iteration on triangular shaped topology on image plane. On the contrary, when HSI scheme is used and each channel is processed separately, the PSNR increased to a lesser extent as noise in image signal does not inherently dependent on the colour scheme. Execution times of the whole process of the entire system have been found to decrease around 8% to 9% for HSI scheme compared to that obtained in RGB scheme. The compression ratio has been found to increase nearly ten times for HSI scheme compared with those obtained in RGB scheme and it holds good for facial images and natural objects and sceneries. The modified HIS scheme has taken up the non linear variation of saturation viz. in sinusoidal, exponential and polynomial form. The overall results have shown that this non linear approach gives higher values of PSNR and processing speed during encoding but with lower values of compression ratio compared to RGB and normal HSI scheme. This has happened due to attaining lower self similarity for non linear change in the saturation in the same image. The present study is expected to provide some new idea about the better applicability of standard and modified HSI scheme compared with traditional RGB colour scheme.

6. References

1. Jacquin AE. A Novel Fractal Block-Coding Technique for Digital Images, *International Conference on Acoustics Speech and Signal Processing.* Albuquerque, NM, 1990; 4:2225-28.
2. Jaquin AE. Image coding based on a fractal theory of iterated contractive image transformations. *IEEE Transactions on Image Processing*. 1992; 1(1):18-30.
3. Barnsley MF. Fractal everywhere, Academic Press: New York, 1988.
4. Fisher Y. Fractal Image compression. Fractals. 1994; 2(3):347-61.
5. Zhang LB, Fan S. New method for fractal image compression based on adaptive threshold value quad tree. *Computer Engineering and Design.* 2006; 27(13):2322-37.
6. Daroine F, Bertin E, Chassery JM. An adaptive partition for fractal image coding. *Fractals*. 1997; 5(1):243-56.
7. Zhu S, Yu L, Bellouata K. An improved fractal image coding algorithm based on adaptive threshold for quad tree partition. *9th The International Society for Optical Engineering*. 2008; 7129:1-8.
8. Li J, Yuan D, Xie Q, Zhang C. Fractal Image Compression by Ant Colony Algorithm. *The 9th International Conference for Young Computer Scientists*, Hunan, 2008, p. 1890-94.
9. Hurtgen B, Stiler C. Fast hierarchical codebook search for fractal coding of still images. *Proceedings of EOS/SPIE Visual Communications PACS Medical Applications'93*, Berlin, 1993, p. 397-408.
10. Thomas L, Deravi F. Region-based fractal image compression using heuristic search. *IEEE Transactions Image Processing.* 1995; 4(6):832-38.
11. Davoine F, Antonini M, Chassery JM, Barlaud M. Fractal image compression based on delauney triangulation and vector quantization. *IEEE Transactions on Image Processing.* 1996; 5(2):338-46.
12. Wenjing L, Wangchao L. A fast fractal image coding technique. *4th International Conference on Signal Processing Proceedings*, ICSP'98, Beijing, 1998, p. 775-78.
13. Polvere M, Nappi M. Speed-up in Fractal Image Coding: Comparison of Methods. *IEEE Transactions on Image Compression*. 2000; 9(6):1002-09.
14. Hamzaoui R, Saupe D, Hiller M. Distortion Minimization with Fast Local Search for Fractal Image Compression. *Journal of Visual Communication and Image Representation*. 2001; 12(4):450-68.
15. Wohlberg B, Jager DG. A Review of the Fractal Image Coding Literature. *IEEE Transactions on Image Processing*. 1999; 8(12):1716-29.

16. Brijmohan B, Yarish Y. Low bit-rate video coding using fractal compression of wavelet sub trees. *7th IEEE Africon Conference in Africa, Gaborone.* 2004; 1:39-44.
17. Zhu ZL, Zhao YL, Yu H. Efficient fractal image compression based on pixels distribution and triangular segmentation. *Journal of computer Applications*. 2010; 30(2):337-40.
18. Ganesan P, Rajini V, Sathish BS, Kalist V, Basha KSK. Satellite Image Segmentation Based on YcbCr Color Space. *Indian Journal of Science and Technology*, 2015 Jan; 8(1):35-41.
19. Kheirkhah E, Tabatabaie ZS. A Hybrid Face Detection Approach in Color Images with Complex Background. *Indian Journal of Science and Technology*. 2015 Jan; 8(1):49-60.
20. Zhao Y, Zhu Z, Yu H. Fractal Color Image Coding Based on Isosceles Triangle Segmentation. *2010 International Workshop on Chaos-Fractal Theory and its Applications*, Kunming, Yunnan, 2010, p. 486-90.
21. Semay N, Hadhoud M, Abdul-Kader H, Abbas A. Noval Compression System for Hue-Saturation and Intensity Color Space. *The International Arab Journal of Information Technology.* 2013; 10(6):546-552.
22. Jayaraman S, Esakkirajan S, Veerakumar T. Digital image processing, 1st edition, Tata McGraw Hill: USA, 2008, p. 1-3.
23. Gonzalez RC, Woods RE. Digital image processing, 3rd edition, Prentice Hall: USA, 2012.
24. Chung KL, Hsu CH. Novel prediction- and sub-block based algorithm for fractal image compression, Chaos. *Solitons and Fractals.* 2006; 29(1):215-22.